

# Pseudo-Time-Varying Admittance Characteristic of Grid-Connected Inverter and Its Corrected Admittance Measurement Method

Xie, Zhiwei; Wu, Wenhua; Chen, Yandong; Guerrero, Josep M.

*Published in:*
IEEE Transactions on Industrial Electronics

*DOI (link to publication from Publisher):*
10.1109/TIE.2021.3099225

*Publication date:*
2022

*Document Version*
Accepted author manuscript, peer reviewed version

This article has been accepted for publication in a future issue of this journal, but has not been fully edited. Content may change prior to final publication. Citation information: DOI 10.1109/TIE.2021.3099225, IEEE Transactions on Industrial Electronics

# Pseudo-Time-Varying Admittance Characteristic of Grid-Connected Inverter and Its Corrected Admittance Measurement Method

Zhiwei Xie, Wenhua Wu, *Member, IEEE*, Yandong Chen, *Senior Member, IEEE*, and Josep M. Guerrero, *Fellow, IEEE*

***Abstract*—When the control parameters and operating conditions remain unchanged, it is usually believed that the admittance characteristic of grid-connected inverter is time-invariant. However, considering the effect of frequency-coupling, an abnormal phenomenon is observed in the admittance measurement of the grid-connected inverter: the phase of the off-diagonal elements $Y_{12}$ and $Y_{21}$ in the admittance matrix is always changed with time, which presents a time-varying admittance characteristic. To explore this phenomenon, the theoretical analyses based on the traditional frequency-coupling admittance measurement method are made. Because the initial phase of the signal cannot be obtained from FFT in experiments and the disturbance frequency and coupling frequency are different, the phase difference between the two frequency components changes with time. However, the influence is not considered in the traditional frequency-coupling admittance measurement method, which makes the measurement results exhibit the confusing time-varying characteristic. The phenomenon is defined as pseudo-time-varying admittance characteristic in this letter. To accurately measure the admittance characteristic of the grid-connected inverter, a frequency-coupling admittance measurement method based on phase correction is proposed, which corrects the phase of disturbance frequency components and coupling frequency components. Finally, the effectiveness of the proposed measurement method is verified by experiments.**

***Index Terms*—Frequency-coupling; grid-connected inverter; pseudo-time-varying admittance characteristic; phase correction.**

## I. Introduction

With the increasing penetration of renewable energy, the interaction between grid-connected inverters and the weak grid becomes more and more intense, which easily causes the system oscillation. Impedance-based method is an effective method to analyze this issue. The impedance (admittance) measurement of the grid-connected inverter is an indispensable part of impedance-based method, which has attracted a lot of attention in recent years.

In terms of sequence impedance measurement method, a sequence impedance measurement method for railway traction power system with controlled-frequency-band is reported in [1]. To avoid the influence of background harmonics and the frequency deviation, an improved measurement method for the grid-connected inverter system is investigated [2]. However, the effect of frequency-coupling in the grid-connected inverter is not considered in the above two methods. If the frequency-coupling is directly ignored in the sequence impedance model, the accuracy of stability analysis will be affected [3].

In order to study the frequency-coupling characteristic of the grid-connected inverter, the admittance of doubly fed induction generator was measured in simulation (Matlab/Simulink) [4]. Further, the frequency-coupling admittance model of grid-connected photovoltaic inverter was verified in simulation [5]. However, it is a pity that the above frequency-coupling characteristic measurements of the grid-connected inverter were not carried in experiment.

In this letter, considering the effect of frequency-coupling, an abnormal phenomenon is observed in the admittance measurement of the grid-connected inverter: phases of the off-diagonal elements $Y_{12}$ and $Y_{21}$ in the admittance matrix are changed with time, which presents a time-varying admittance characteristic. The existing frequency-coupling admittance measurement methods of the grid-connected inverter have not reported this abnormal phenomenon [4]-[6]. This letter focuses on this phenomenon, explores its root causes, and puts forward a frequency-coupling admittance measurement method based on phase correction to avoid it. Simulation and experiment verify the correctness of the analysis and the proposed measurement method.

## II. The Phenomenon of Pseudo-time-varying Admittance Characteristic

### A. The traditional frequency-coupling admittance measurement method

The measured grid-connected inverter is shown in Fig. 1 and its frequency-coupling admittance model is defined as (1). When the admittance characteristic is to be measured, the small-disturbance voltage $v_{dis}$ at the designed frequency should be injected into the point of common coupling. The admittance at $f_p$ can be calculated with the extracted voltage responses and current responses at the disturbance frequency $f_p$ and coupling frequency $f_{p1} = f_p - 2f_1$ in $v_a$, $v_b$, $v_c$, $i_a$, $i_b$, and $i_c$.

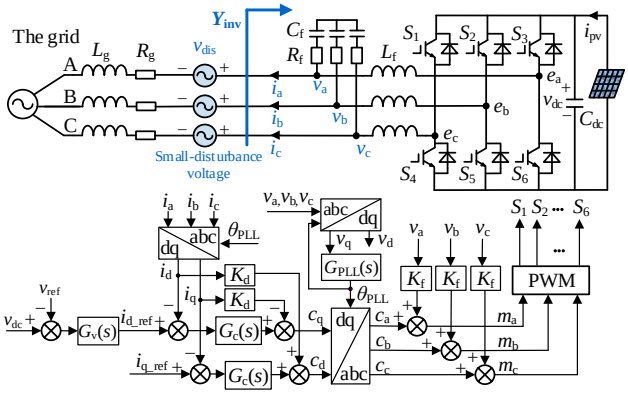


**Fig. 1 Topology and control scheme of the measured grid-connected inverter.**

$$-\begin{bmatrix}\mathbf{I}_p\\ \mathbf{I}_{p1}\end{bmatrix}=\begin{bmatrix}Y_{11} & Y_{12}\\ Y_{21} & Y_{22}\end{bmatrix}\begin{bmatrix}\mathbf{V}_p\\ \mathbf{V}_{p1}\end{bmatrix} \tag{1}$$

where $\mathbf{I}_p$ and $\mathbf{I}_{p1}$ presents the response currents at $f_p$ and $f_{p1}$, $\mathbf{V}_p$ and $\mathbf{V}_{p1}$ presents the response voltages at $f_p$ and $f_{p1}$, respectively.

Manuscript received January 28, 2021; revised June 9, 2021; accepted July 10, 2021. This work was supported in part by the Natural Science Foundation of China (NSFC) (52007058, 52077070).

Z. Xie, and Y. Chen are with the College of Electrical and Information Engineering, Hunan University, Changsha 410082, China (e-mail: xiezhiwei@hnu.edu.cn; yandong_chen@hnu.edu.cn).

W. Wu is with the College of Electrical and Information Engineering, Hunan University, Changsha 410082, China (Corresponding author, e-mail: wuwenhua168@hnu.edu.cn).

J. M. Guerrero is with the Department of Energy Technology, Aalborg University, Denmark. (e-mail: joz@et.aau.dk).

This article has been accepted for publication in a future issue of this journal, but has not been fully edited. Content may change prior to final publication. Citation information: DOI 10.1109/TIE.2021.3099225, IEEE Transactions on Industrial Electronics

There are two equations with four variables in (1). Thus, it is necessary to inject two linear independent small-disturbance voltages into the measured system to calculate the four variables:

$$\begin{cases} Y_{11}=\dfrac{\mathbf{I}_p^{'}\times\mathbf{V}_{p1}^{''}-\mathbf{V}_{p1}^{'}\times\mathbf{I}_p^{''}}{\mathbf{V}_p^{''}\times\mathbf{V}_{p1}^{'}-\mathbf{V}_p^{'}\times\mathbf{V}_{p1}^{''}}, & Y_{12}=\dfrac{\mathbf{V}_p^{'}\times\mathbf{I}_p^{''}-\mathbf{I}_p^{'}\times\mathbf{V}_p^{''}}{\mathbf{V}_p^{''}\times\mathbf{V}_{p1}^{'}-\mathbf{V}_p^{'}\times\mathbf{V}_{p1}^{''}} \\ Y_{21}=\dfrac{\mathbf{I}_{p1}^{'}\times\mathbf{V}_{p1}^{''}-\mathbf{I}_{p1}^{''}\times\mathbf{V}_{p1}^{'}}{\mathbf{V}_p^{''}\times\mathbf{V}_{p1}^{'}-\mathbf{V}_p^{'}\times\mathbf{V}_{p1}^{''}}, & Y_{22}=\dfrac{\mathbf{V}_p^{'}\times\mathbf{I}_{p1}^{''}-\mathbf{I}_{p1}^{'}\times\mathbf{V}_p^{''}}{\mathbf{V}_p^{''}\times\mathbf{V}_{p1}^{'}-\mathbf{V}_p^{'}\times\mathbf{V}_{p1}^{''}} \end{cases} \quad (2)$$

where the superscript " ' " and " " " represent the response of the measured system after the first injection and the second injection.

According to (2), the key steps of the traditional frequency-coupling admittance measurement method are shown in Fig. 2.

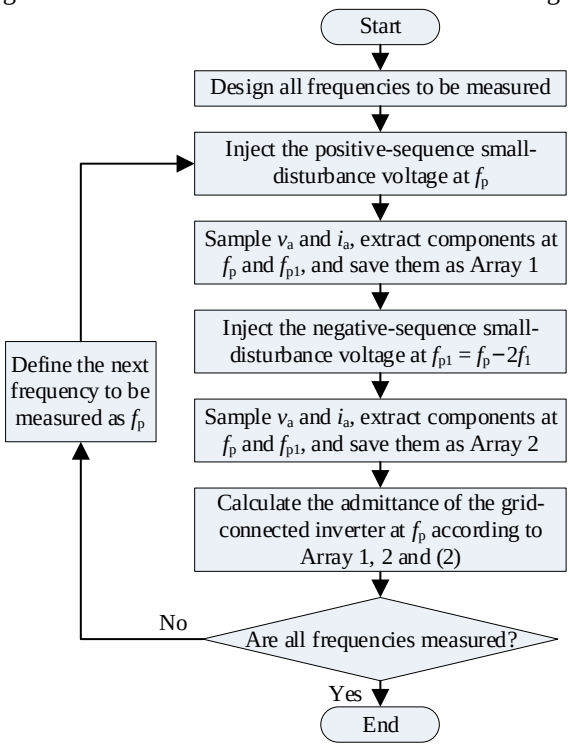


**Fig. 2 The traditional frequency-coupling admittance measurement method.**

### *B. Pseudo-time-varying admittance characteristic in experiments*

The experimental measurement results with the traditional measurement method are shown in Fig. 3. The phase measurement results of $Y_{12}$ and $Y_{21}$ are in disorder. In addition, the phase measurement results of $Y_{12}$ and $Y_{21}$ is different every time, which makes $Y_{12}$ and $Y_{21}$ appear to be time-varying.

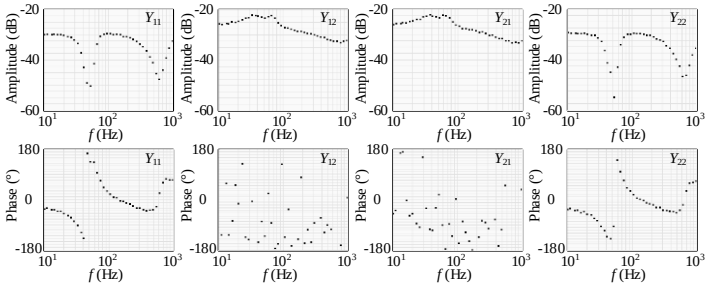


**Fig. 3 Experimental results of admittance measurement.**

### *C. Pseudo-time-varying admittance characteristic in simulations*

The traditional admittance measurement method is also used in Matlab/Simulink simulation. Different from the experiment, in a broadband admittance measurement simulation, the sampling can start from the same simulation time $t_0$ at each measured frequency.

Fig. 4 shows the several simulation results of admittance measurement of the grid-connected inverter under different $t_0$. When $t_0$ is changed from 1.000s to 1.004s, the measurement results gradually deviate from the theoretical model; when $t_0$ is changed from 1.006s to 1.010s, the measurement results gradually approach the theoretical model until they are consistent with the theoretical model again. The phase characteristics of $Y_{12}$ and $Y_{21}$ change with $t_0$.

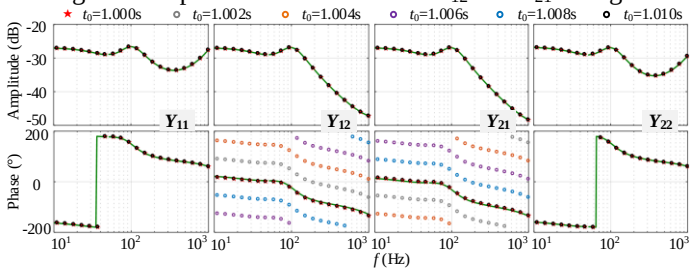


**Fig. 4 Simulation results of admittance measurement under different $t_0$.**

In a broadband admittance measurement experiment, the sampling start time $t_0$ is random at each measured frequency. It can be speculated that the disordered phase measurement results of $Y_{12}$ and $Y_{21}$ in Fig. 3 are caused by the difference of $t_0$.

The admittance measurement results of the grid-connected inverter will appear to have time-varying characteristic no matter in experiment or simulation. However, this characteristic is not consistent with the theoretical model. Thus, this abnormal phenomenon is defined as pseudo time-varying admittance characteristic.

## III. The Root Causes of Pseudo-time-varying Admittance Characteristic

When the admittance of the grid-connected inverter at $f_p$ is measured, the positive-sequence small-disturbance voltage at $f_p$ and the negative-sequence small-disturbance voltage at $f_{p1}$ are injected into the system respectively to obtain the responses in (2). The time domain expressions of $v_a$ and $i_a$ after the first injection at $f_p$ and the second injection at $f_{p1}$ are respectively shown as (3)-(4) with the sampling start time $t_0^{'}$ and (5)-(6) with the sampling start time $t_0^{''}$.

$$v_a^{'}=V_1\cos\left(2\pi f_1 t_0^{'}\right)+V_p^{'}\cos\left(2\pi f_p t_0^{'}+\varphi_{vp}^{'}\right)+V_{p1}^{'}\cos\left(2\pi f_{p1} t_0^{'}+\varphi_{vp1}^{'}\right) \quad (3)$$

$$i_a^{'}=I_1\cos\left(2\pi f_1 t_0^{'}+\varphi_{i1}\right)+I_p^{'}\cos\left(2\pi f_p t_0^{'}+\varphi_{ip}^{'}\right)+I_{p1}^{'}\cos\left(2\pi f_{p1} t_0^{'}+\varphi_{ip1}^{'}\right) \quad (4)$$

$$v_a^{''}=V_1\cos\left(2\pi f_1 t_0^{''}\right)+V_p^{''}\cos\left(2\pi f_p t_0^{''}+\varphi_{vp}^{''}\right)+V_{p1}^{''}\cos\left(2\pi f_{p1} t_0^{''}+\varphi_{vp1}^{''}\right) \quad (5)$$

$$i_a^{''}=I_1\cos\left(2\pi f_1 t_0^{''}+\varphi_{i1}\right)+I_p^{''}\cos\left(2\pi f_p t_0^{''}+\varphi_{ip}^{''}\right)+I_{p1}^{''}\cos\left(2\pi f_{p1} t_0^{''}+\varphi_{ip1}^{''}\right) \quad (6)$$

where $\varphi_{vp}$ and $\varphi_{vp1}$ are the initial phases of voltage components at $f_p$ and $f_{p1}$, and $\varphi_{i1}$, $\varphi_{ip}$ and $\varphi_{ip1}$ are the initial phases of current components at fundamental frequency $f_1$, $f_p$ and $f_{p1}$, respectively.

The phase obtained from FFT is the phase of cosine signal at the beginning of sampling. Therefore, the phase changes all the time with the different $t_0$ ($t_0^{'}$ or $t_0^{''}$), as shown in Fig. 5.

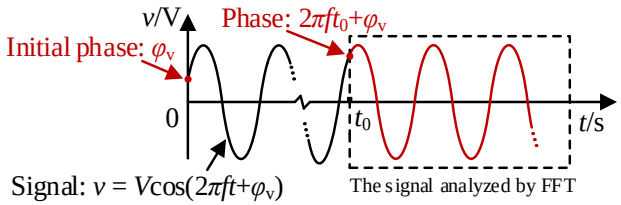


**Fig. 5 Schematic diagram of the phase obtained from FFT.**

According to the time domain expressions of phase voltage and current in (3)-(6), (2) can be written as (7). After further simplifying, (8) can be obtained. The red parts marked in (8) are the time-varying phases related to the sampling start time $t_0^{'}$ and $t_0^{''}$. The admittance phases are changing with the sampling start time. The admittance phase will exhibit the confusing time-varying characteristic, when the frequency-coupling admittance measurement of the grid-connected inverter is carried out based on FFT.

This article has been accepted for publication in a future issue of this journal, but has not been fully edited. Content may change prior to final publication. Citation information: DOI 10.1109/TIE.2021.3099225, IEEE Transactions on Industrial Electronics

$$\begin{cases} Y_{11}=\dfrac{I_{\mathrm{p}}^{'}\angle\left(2\pi f_{\mathrm{p}}t_0^{'}+\varphi_{\mathrm{ip}}^{'}\right)\cdot V_{\mathrm{p1}}^{''}\angle\left(2\pi f_{\mathrm{p1}}t_0^{''}+\varphi_{\mathrm{vp1}}^{''}\right)-V_{\mathrm{p1}}^{'}\angle\left(2\pi f_{\mathrm{p1}}t_0^{'}+\varphi_{\mathrm{vp1}}^{'}\right)\cdot I_{\mathrm{p}}^{''}\angle\left(2\pi f_{\mathrm{p}}t_0^{''}+\varphi_{\mathrm{ip}}^{''}\right)}{V_{\mathrm{p}}^{''}\angle\left(2\pi f_{\mathrm{p}}t_0^{''}+\varphi_{\mathrm{vp}}^{''}\right)\cdot V_{\mathrm{p1}}^{'}\angle\left(2\pi f_{\mathrm{p1}}t_0^{'}+\varphi_{\mathrm{vp1}}^{'}\right)-V_{\mathrm{p}}^{'}\angle\left(2\pi f_{\mathrm{p}}t_0^{'}+\varphi_{\mathrm{vp}}^{'}\right)\cdot V_{\mathrm{p1}}^{''}\angle\left(2\pi f_{\mathrm{p1}}t_0^{''}+\varphi_{\mathrm{vp1}}^{''}\right)} \\ Y_{12}=\dfrac{V_{\mathrm{p}}^{'}\angle\left(2\pi f_{\mathrm{p}}t_0^{'}+\varphi_{\mathrm{vp}}^{'}\right)\cdot I_{\mathrm{p}}^{''}\angle\left(2\pi f_{\mathrm{p}}t_0^{''}+\varphi_{\mathrm{ip}}^{''}\right)-I_{\mathrm{p}}^{'}\angle\left(2\pi f_{\mathrm{p}}t_0^{'}+\varphi_{\mathrm{ip}}^{'}\right)\cdot V_{\mathrm{p}}^{''}\angle\left(2\pi f_{\mathrm{p}}t_0^{''}+\varphi_{\mathrm{vp}}^{''}\right)}{V_{\mathrm{p}}^{''}\angle\left(2\pi f_{\mathrm{p}}t_0^{''}+\varphi_{\mathrm{vp}}^{''}\right)\cdot V_{\mathrm{p1}}^{'}\angle\left(2\pi f_{\mathrm{p1}}t_0^{'}+\varphi_{\mathrm{vp1}}^{'}\right)-V_{\mathrm{p}}^{'}\angle\left(2\pi f_{\mathrm{p}}t_0^{'}+\varphi_{\mathrm{vp}}^{'}\right)\cdot V_{\mathrm{p1}}^{''}\angle\left(2\pi f_{\mathrm{p1}}t_0^{''}+\varphi_{\mathrm{vp1}}^{''}\right)} \\ Y_{21}=\dfrac{I_{\mathrm{p1}}^{'}\angle\left(2\pi f_{\mathrm{p1}}t_0^{'}+\varphi_{\mathrm{ip1}}^{'}\right)\cdot V_{\mathrm{p1}}^{''}\angle\left(2\pi f_{\mathrm{p1}}t_0^{''}+\varphi_{\mathrm{vp1}}^{''}\right)-I_{\mathrm{p1}}^{''}\angle\left(2\pi f_{\mathrm{p1}}t_0^{''}+\varphi_{\mathrm{ip1}}^{''}\right)\cdot V_{\mathrm{p1}}^{'}\angle\left(2\pi f_{\mathrm{p1}}t_0^{'}+\varphi_{\mathrm{vp1}}^{'}\right)}{V_{\mathrm{p}}^{''}\angle\left(2\pi f_{\mathrm{p}}t_0^{''}+\varphi_{\mathrm{vp}}^{''}\right)\cdot V_{\mathrm{p1}}^{'}\angle\left(2\pi f_{\mathrm{p1}}t_0^{'}+\varphi_{\mathrm{vp1}}^{'}\right)-V_{\mathrm{p}}^{'}\angle\left(2\pi f_{\mathrm{p}}t_0^{'}+\varphi_{\mathrm{vp}}^{'}\right)\cdot V_{\mathrm{p1}}^{''}\angle\left(2\pi f_{\mathrm{p1}}t_0^{''}+\varphi_{\mathrm{vp1}}^{''}\right)} \\ Y_{22}=\dfrac{V_{\mathrm{p}}^{'}\angle\left(2\pi f_{\mathrm{p}}t_0^{'}+\varphi_{\mathrm{vp}}^{'}\right)\cdot I_{\mathrm{p1}}^{''}\angle\left(2\pi f_{\mathrm{p1}}t_0^{''}+\varphi_{\mathrm{ip1}}^{''}\right)-I_{\mathrm{p1}}^{'}\angle\left(2\pi f_{\mathrm{p1}}t_0^{'}+\varphi_{\mathrm{ip1}}^{'}\right)\cdot V_{\mathrm{p}}^{''}\angle\left(2\pi f_{\mathrm{p}}t_0^{''}+\varphi_{\mathrm{vp}}^{''}\right)}{V_{\mathrm{p}}^{''}\angle\left(2\pi f_{\mathrm{p}}t_0^{''}+\varphi_{\mathrm{vp}}^{''}\right)\cdot V_{\mathrm{p1}}^{'}\angle\left(2\pi f_{\mathrm{p1}}t_0^{'}+\varphi_{\mathrm{vp1}}^{'}\right)-V_{\mathrm{p}}^{'}\angle\left(2\pi f_{\mathrm{p}}t_0^{'}+\varphi_{\mathrm{vp}}^{'}\right)\cdot V_{\mathrm{p1}}^{''}\angle\left(2\pi f_{\mathrm{p1}}t_0^{''}+\varphi_{\mathrm{vp1}}^{''}\right)} \end{cases} \tag{7}$$

$$\begin{cases} Y_{11}=\dfrac{I_{\mathrm{p}}^{'}\cdot V_{\mathrm{p1}}^{''}\angle\left(-4\pi f_1t_0^{''}+\varphi_{\mathrm{ip}}^{'}+\varphi_{\mathrm{vp1}}^{''}\right)-V_{\mathrm{p1}}^{'}\cdot I_{\mathrm{p}}^{''}\angle\left(-4\pi f_1t_0^{'}+\varphi_{\mathrm{vp1}}^{'}+\varphi_{\mathrm{ip}}^{''}\right)}{V_{\mathrm{p}}^{''}\cdot V_{\mathrm{p1}}^{'}\angle\left(-4\pi f_1t_0^{'}+\varphi_{\mathrm{vp}}^{''}+\varphi_{\mathrm{vp1}}^{'}\right)-V_{\mathrm{p}}^{'}\cdot V_{\mathrm{p1}}^{''}\angle\left(-4\pi f_1t_0^{''}+\varphi_{\mathrm{vp}}^{'}+\varphi_{\mathrm{vp1}}^{''}\right)} \\ Y_{12}=\dfrac{V_{\mathrm{p}}^{'}\cdot I_{\mathrm{p}}^{''}\angle\left(\varphi_{\mathrm{vp}}^{'}+\varphi_{\mathrm{ip}}^{''}\right)-I_{\mathrm{p}}^{'}\cdot V_{\mathrm{p}}^{''}\angle\left(\varphi_{\mathrm{ip}}^{'}+\varphi_{\mathrm{vp}}^{''}\right)}{V_{\mathrm{p}}^{''}\cdot V_{\mathrm{p1}}^{'}\angle\left(-4\pi f_1t_0^{'}+\varphi_{\mathrm{vp}}^{''}+\varphi_{\mathrm{vp1}}^{'}\right)-V_{\mathrm{p}}^{'}\cdot V_{\mathrm{p1}}^{''}\angle\left(-4\pi f_1t_0^{''}+\varphi_{\mathrm{vp}}^{'}+\varphi_{\mathrm{vp1}}^{''}\right)} \\ Y_{21}=\dfrac{\left[I_{\mathrm{p1}}^{'}\cdot V_{\mathrm{p1}}^{''}\angle\left(\varphi_{\mathrm{ip1}}^{'}+\varphi_{\mathrm{vp1}}^{''}\right)-I_{\mathrm{p1}}^{''}\cdot V_{\mathrm{p1}}^{'}\angle\left(\varphi_{\mathrm{ip1}}^{''}+\varphi_{\mathrm{vp1}}^{'}\right)\right]\angle\left[-4\pi f_1\left(t_0^{'}+t_0^{''}\right)\right]}{V_{\mathrm{p}}^{''}\cdot V_{\mathrm{p1}}^{'}\angle\left(-4\pi f_1t_0^{'}+\varphi_{\mathrm{vp}}^{''}+\varphi_{\mathrm{vp1}}^{'}\right)-V_{\mathrm{p}}^{'}\cdot V_{\mathrm{p1}}^{''}\angle\left(-4\pi f_1t_0^{''}+\varphi_{\mathrm{vp}}^{'}+\varphi_{\mathrm{vp1}}^{''}\right)} \\ Y_{22}=\dfrac{V_{\mathrm{p}}^{'}\cdot I_{\mathrm{p1}}^{''}\angle\left(-4\pi f_1t_0^{''}+\varphi_{\mathrm{vp}}^{'}+\varphi_{\mathrm{ip1}}^{''}\right)-I_{\mathrm{p1}}^{'}\cdot V_{\mathrm{p}}^{''}\angle\left(-4\pi f_1t_0^{'}+\varphi_{\mathrm{ip1}}^{'}+\varphi_{\mathrm{vp}}^{''}\right)}{V_{\mathrm{p}}^{''}\cdot V_{\mathrm{p1}}^{'}\angle\left(-4\pi f_1t_0^{'}+\varphi_{\mathrm{vp}}^{''}+\varphi_{\mathrm{vp1}}^{'}\right)-V_{\mathrm{p}}^{'}\cdot V_{\mathrm{p1}}^{''}\angle\left(-4\pi f_1t_0^{''}+\varphi_{\mathrm{vp}}^{'}+\varphi_{\mathrm{vp1}}^{''}\right)} \end{cases} \tag{8}$$

Considering the relationship between voltage and current in the grid-connected inverter system, the response voltage at the coupling frequency ($\mathbf{V}_{\mathrm{p1}}^{'}$ and $\mathbf{V}_{\mathrm{p}}^{''}$) generates from the response current at the coupling frequency ($\mathbf{I}_{\mathrm{p1}}^{'}$ and $\mathbf{I}_{\mathrm{p}}^{''}$) and the grid impedance. Due to the grid impedance is relatively small to the measured grid-connected inverter, the amplitude of the response voltage at the coupling frequency ($\mathbf{V}_{\mathrm{p1}}^{'}$ and $\mathbf{V}_{\mathrm{p}}^{''}$) is much smaller than that of the response voltage at the disturbance frequency ($\mathbf{V}_{\mathrm{p}}^{'}$ and $\mathbf{V}_{\mathrm{p1}}^{''}$). What's more, as for the measured grid-connected inverter in this letter, the response current at the disturbance frequency is equal to or greater than the response current at the coupling frequency. Therefore, (8) can be simplified as (9) in this condition. (9) shows that the phase of $Y_{12}$ is mainly influenced with $t_0^{''}$ and the phase of $Y_{21}$ is mainly influenced with $t_0^{'}$ while the phases of $Y_{11}$ and $Y_{22}$ are less affected by the sampling start time, which can be ignored. When the fundamental frequency of the grid voltage $f_1$ = 50 Hz, phases of $Y_{12}$ and $Y_{21}$ change gradually with a period of 0.01s. It is consistent with Fig. 3 and Fig. 4.

$$\begin{cases} Y_{11}\approx\dfrac{I_{\mathrm{p}}^{'}\cdot V_{\mathrm{p1}}^{''}\angle\left(\varphi_{\mathrm{ip}}^{'}+\varphi_{\mathrm{vp1}}^{''}\right)}{-V_{\mathrm{p}}^{'}\cdot V_{\mathrm{p1}}^{''}\angle\left(\varphi_{\mathrm{vp}}^{'}+\varphi_{\mathrm{vp1}}^{''}\right)} \\ Y_{12}\approx\dfrac{V_{\mathrm{p}}^{'}\cdot I_{\mathrm{p}}^{''}\angle\left(\varphi_{\mathrm{vp}}^{'}+\varphi_{\mathrm{ip}}^{''}\right)-I_{\mathrm{p}}^{'}\cdot V_{\mathrm{p}}^{''}\angle\left(\varphi_{\mathrm{ip}}^{'}+\varphi_{\mathrm{vp}}^{''}\right)}{-V_{\mathrm{p}}^{'}\cdot V_{\mathrm{p1}}^{''}\angle\left(-4\pi f_1t_0^{''}+\varphi_{\mathrm{vp}}^{'}+\varphi_{\mathrm{vp1}}^{''}\right)} \\ Y_{21}\approx\dfrac{\left[I_{\mathrm{p1}}^{'}\cdot V_{\mathrm{p1}}^{''}\angle\left(\varphi_{\mathrm{ip1}}^{'}+\varphi_{\mathrm{vp1}}^{''}\right)-I_{\mathrm{p1}}^{''}\cdot V_{\mathrm{p1}}^{'}\angle\left(\varphi_{\mathrm{ip1}}^{''}+\varphi_{\mathrm{vp1}}^{'}\right)\right]\angle\left(-4\pi f_1t_0^{'}\right)}{-V_{\mathrm{p}}^{'}\cdot V_{\mathrm{p1}}^{''}\angle\left(\varphi_{\mathrm{vp}}^{'}+\varphi_{\mathrm{vp1}}^{''}\right)} \\ Y_{22}\approx\dfrac{V_{\mathrm{p}}^{'}\cdot I_{\mathrm{p1}}^{''}\angle\left(\varphi_{\mathrm{vp}}^{'}+\varphi_{\mathrm{ip1}}^{''}\right)}{-V_{\mathrm{p}}^{'}\cdot V_{\mathrm{p1}}^{''}\angle\left(\varphi_{\mathrm{vp}}^{'}+\varphi_{\mathrm{vp1}}^{''}\right)} \end{cases} \tag{9}$$

From the above analysis, the root causes of this abnormal phenomenon can be concluded as: 1) the phase obtained from FFT is the phase of cosine signal at $t_0$, rather than the initial phase of the signal; 2) because of the frequency-coupling, the frequencies in the numerator and denominator of $Y_{12}$ and $Y_{21}$ are different, which makes $t_0$ has impact on the phase of $Y_{12}$ and $Y_{21}$.

## IV. The Frequency-Coupling Admittance Measurement Method Based on Phase Correction

In the process of admittance theoretical modeling for the grid-connected inverter, the amplitude, frequency, and initial phase of signal are directly used for derivation. Therefore, the theoretical model is only affected by the initial phase of signal, and is independent on the phase determined by the sampling start time. For the grid-connected inverters with other different control strategies, the relationship between voltage and current under disturbance frequency and coupling frequency may be different from that of the measured grid-connected inverter in this letter, and (9) may not be obtained. Therefore, in order to accurately measure the frequency-coupling admittance of the grid-connected inverter, the initial phase of phase voltage and current should be obtained, or the influence of the time-varying part in $Y_{11}$, $Y_{12}$, $Y_{21}$, and $Y_{22}$ as shown in (8) need to be eliminated.

Because the initial phase is the phase of the signal at $t$ = 0s, the initial phase cannot be obtained through FFT in experiments. However, when phases of time-varying parts of $Y_{11}$, $Y_{12}$, $Y_{21}$, and $Y_{22}$ are $2k\pi$ ($k \in$ Z, Z is an integer set), the time-varying part has no effect on the phase measurement results of $Y_{11}$, $Y_{12}$, $Y_{21}$, and $Y_{22}$. Therefore, in order to eliminate the influence of time-varying parts in phases of $Y_{11}$, $Y_{12}$, $Y_{21}$, and $Y_{22}$, the time-varying parts should satisfy the following conditions

$$-4\pi f_1t_0^{'}=2k_1\pi,\ k_1\in\mathrm{Z};\quad -4\pi f_1t_0^{''}=2k_2\pi,\ k_2\in\mathrm{Z} \tag{10}$$

Considering that $t_0^{'}\geq$ 0s, $t_0^{''}\geq$ 0s, (10) can be solved as

$$\begin{cases} t_0^{'}=k_1/(2f_1)=T_1\cdot k_1/2,\quad k_1\in\mathrm{N} \\ t_0^{''}=k_2/(2f_1)=T_1\cdot k_2/2,\quad k_2\in\mathrm{N} \end{cases} \tag{11}$$

where N is the set of natural numbers; $T_1 = 1/f_1$.

According to (11), if $t_0^{'}$ and $t_0^{''}$ is the time of peak or trough of the fundamental voltage, the time-varying parts of $Y_{11}$, $Y_{12}$, $Y_{21}$, and $Y_{22}$ in (8) will not affect the admittance measurement results. Thus, the admittance of the grid-connected inverter considering the effect of frequency-coupling can be accurately measured.

Due to the influence of harmonics and other frequency components, the voltage waveform of the grid is easily distorted, and it is difficult to accurately start sampling from the peak or trough of the fundamental voltage. In this letter, a frequency-coupling admittance measurement method based on phase correction is proposed. No matter what $t_0^{'}$ and $t_0^{''}$ is, the phases of voltage and current components whose frequencies are $f_{\mathrm{p}}$ or $f_{\mathrm{p1}}$ can be corrected by the phase of fundamental voltage. This method has the same effect as $t_0$ selected at the peak of fundamental voltage.

Taking disturbance voltage $v_{\mathrm{p}}$ as an example, the principle of phase correction in the proposed measurement method is shown in Fig. 6. The phase of the fundamental voltage ($v_1$ in Fig. 6) at the peak is zero. Therefore, the phase at $t = k/f_1$ is selected as the reference phase. After the small-disturbance voltage is injected and the

This article has been accepted for publication in a future issue of this journal, but has not been fully edited. Content may change prior to final publication. Citation information: DOI 10.1109/TIE.2021.3099225, IEEE Transactions on Industrial Electronics

system returns stable, the signal with the time length $T_{ff}$ is sampled from $t_0$. Based on the sampled signal, the phase of fundamental voltage $\varphi_{v1\_m}$ and the phase of disturbance voltage $\varphi_{vp\_m}$ can be obtained from FFT. Subtracting the phase of $v_p$ changed in time $t_{cor}$ from $\varphi_{vp\_m}$, the phase of $v_p$ at $t_0$ can be corrected to $t = k/f_1$. After correction, the phase of $v_p$ at $t = k/f_1$ is $\varphi_{vp\_c}$.

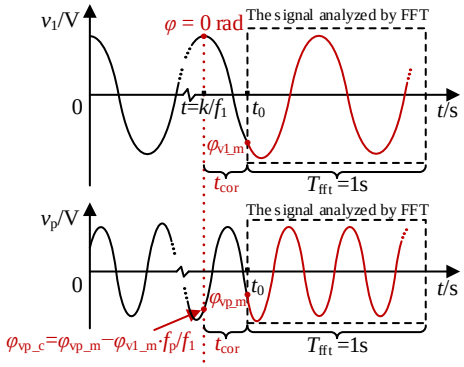


**Fig. 6 The principle of phase correction in the proposed measurement method.**

$$\begin{cases} t_{cor} = \varphi_{v1\_m} / 2\pi \cdot (1/f_1) \\ \varphi_{vp\_c} = \varphi_{vp\_m} - t_{cor} / (1/f_p) \cdot 2\pi = \varphi_{vp\_m} - \varphi_{v1\_m} \cdot (f_p / f_1) \end{cases} \tag{12}$$

Similarly, corrected phase $\varphi_{vp1\_c}$, $\varphi_{ip1\_c}$ and $\varphi_{ip\_c}$ of $v_{p1}$, $i_{p1}$ and $i_p$ can be obtained as

$$\begin{cases} \varphi_{vp1\_c} = \varphi_{vp1\_m} - \varphi_{v1\_m} \cdot (f_{p1} / f_1) \\ \varphi_{ip1\_c} = \varphi_{ip1\_m} - \varphi_{v1\_m} \cdot (f_{p1} / f_1) \\ \varphi_{ip\_c} = \varphi_{ip\_m} - \varphi_{v1\_m} \cdot (f_p / f_1) \end{cases} \tag{13}$$

where $\varphi_{vp1\_m}$, $\varphi_{ip1\_m}$, and $\varphi_{ip\_m}$ is the phase of $v_{p1}$, $i_{p1}$ and $i_p$ at $t_0$.

Compared with the traditional measurement method, the proposed measurement method needs to make a phase correction before extracting the components at $f_p$ and $f_{p1}$ in $v_a$ and $i_a$. Therefore, the specific steps of the proposed frequency-coupling admittance measurement method based on phase correction are concluded as follows.

1) After the small-disturbance voltage for the first time is injected and the system returns stable, the signal with the time length $T_{ff}$ is sampled from $t'_0$. $V_p' \angle (\varphi'_{vp\_m})$, $V_{p1}' \angle (\varphi'_{vp1\_m})$, $I_p' \angle (\varphi'_{ip\_m})$, $I_{p1}' \angle (\varphi'_{ip1\_m})$ and $V_1 \angle (\varphi'_{v1\_m})$ can be obtained from FFT.

2) The phases of the disturbance component and the coupling component are corrected according to (12)-(13). $V_p' \angle (\varphi'_{vp\_c})$, $V_{p1}' \angle (\varphi'_{vp1\_c})$, $I_p' \angle (\varphi'_{ip\_c})$ and $I_{p1}' \angle (\varphi'_{ip1\_c})$ are obtained.

3) After the small-disturbance voltage for the second time is injected and the system returns stable, repeat the first step to the second step. $V_p'' \angle (\varphi''_{vp\_c})$, $V_{p1}'' \angle (\varphi''_{vp1\_c})$, $I_p'' \angle (\varphi''_{ip\_c})$, $I_{p1}'' \angle (\varphi''_{ip1\_c})$ and $V_1 \angle (\varphi''_{v1\_m})$ are obtained. The frequency-coupling admittance of the grid-connected inverter at $f_p$ can be calculated from (2).

4) Repeat the first step to the third step until the frequency-coupling admittance of the grid-connected inverter at all design frequencies are measured.

## V. Experimental Verification

To verify the correctness of the theoretical analysis and the proposed frequency-coupling admittance measurement method, the admittance measurement of the grid-connected inverter considering the effect of frequency-coupling is carried out on the admittance measurement experimental platform in Fig. 7 with the proposed measurement method. The photovoltaic array simulator can work as the photovoltaic and is able to operate in constant current mode. Additionally, the Hanning window, the interpolation method, and the small-disturbance injection method with shifting frequency are adopted in the admittance measurement to mitigate the influence of the grid frequency deviation and background harmonics. The selected theoretical model has considered the influence of frequency-coupling, the DC-side control, DC-side capacitor, the phase-locked loop, the AC-side control and the control delay to describe the measured grid-connected inverter more accurately. The experimental parameters are consistent with the simulation.

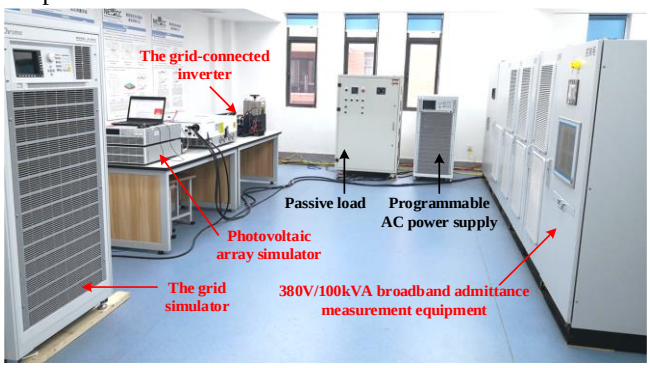


**Fig. 7 The admittance measurement experimental platform.**

The experimental measurement results are shown in Fig. 8, which are consistent with the previous theoretical model. Compared with Fig. 3, the experimental measurement results in Fig. 8 verify the effectiveness of the proposed frequency-coupling admittance measurement method based on phase correction.

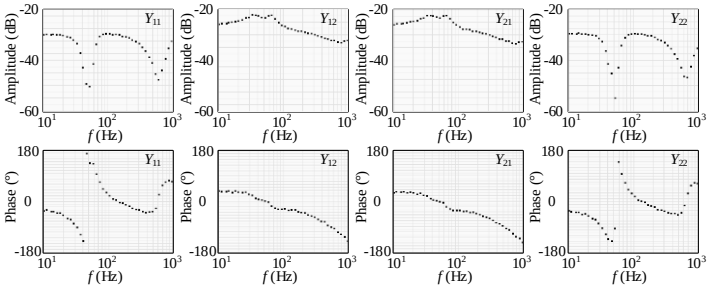


**Fig. 8 The measurement results with the proposed measurement method.**

## VI. Conclusions

In this letter, the pseudo-time-varying admittance characteristic of the grid-connected inverter are reported. The root causes for this abnormal phenomenon are that the initial phase of the signal cannot be obtained from FFT in experiments and the frequencies in the numerator and denominator terms of $Y_{12}$ and $Y_{21}$ are different. To avoid this abnormal phenomenon, a frequency-coupling admittance measurement method based on phase correction is proposed, which can accurately measure the frequency-coupling admittance.

## References

[1] P. Pan, H. Hu, D. Xiao, Y. Song and Z. He, "An improved controlled-frequency-band impedance measurement scheme for railway traction power system," *IEEE Trans. Ind. Electron.*, vol. 68, no. 3, pp. 2184-2195, Mar. 2021.

[2] P. Zhong, J. Sun, Z. Tian, M. Huang, P. Yu, and X. Zha, "An improved impedance measurement method for grid-connected inverter systems considering the background harmonics and frequency deviation," *IEEE J. Emerg. Sel. Topics Power Electron.*, early access.

[3] M. Bakhshizadeh, X. Wang, F. Blaabjerg, J. Hjerrild, Ł. Kocewiak, C. Bak, et al. "Couplings in phase domain impedance modeling of grid-connected converters," *IEEE Trans. Power Electron.*, vol. 31, no. 10, pp. 6792-6795, Oct. 2016.

[4] Y. Xu, H. Nian, T. Wang, L. Chen, and T. Zheng, "Frequency coupling characteristic modeling and stability analysis of doubly fed induction generator," *IEEE Trans. Energy Convers.*, vol. 33, no. 3, pp. 1475-1486, Sep. 2018.

[5] B. Zhang, X. Du, J. Zhao, J. Zhou and X. Zou, "Impedance modeling and stability analysis of a three-phase three-level NPC inverter connected to the grid," in *CSEE J. Power Energy*, vol. 6, no. 2, pp. 270-278, Jun. 2020.

[6] S. Shah, P. Koralewicz, V. Gevorgian, and R. Wallen, "Impedance measurement of wind turbines using a multimegawatt grid simulator," in *18th Wind Integration Workshop*, Dublin, Ireland, Oct.2019, pp. 1-6.